CN(A2iX2+) and CN(B2+X2+) yields from HCN photodissociation

L. C. Lee

Citation: J. Chem. Phys. **72**, 6414 (1980); doi: 10.1063/1.439140
View online: http://dx.doi.org/10.1063/1.439140
View Table of Contents: http://jcp.aip.org/resource/1/JCPSA6/v72/i12
Published by the American Institute of Physics.

CN($A\,^2\Pi_i \rightarrow X\,^2\Sigma^+$) and CN($B\,^2\Sigma^+ \rightarrow X\,^2\Sigma^+$) yields from HCN photodissociation

L. C. Lee

Molecular Physics Laboratory, SRI International, Menlo Park, California 94025
(Received 22 October 1979; accepted 4 March 1980)

The cross sections for the production of CN($A\,^2\Pi_i \rightarrow X\,^2\Sigma^+$) and CN($B\,^2\Sigma^+ \rightarrow X\,^2\Sigma^+$) emissions from HCN photodissociation are measured using synchrotron radiation in the 1050–1550 Å region. The photoabsorption cross section of HCN is also measured, and the quantum yields for the emissions are determined. The spectra for the photoabsorption and photoemission cross sections are interpreted with the known excited states of HCN. Three new excited states are found from the CN emission quantum yields. It is observed that the vibrational population of the CN($B\,^2\Sigma^+$) photofragments produced by photodissociating HCN at Rydberg states are more vibrationally excited than those produced at other dissociative states. The photodissociation processes for producing CN emissions at various excited states are discussed.

I. INTRODUCTION

Hydrogen cyanide molecules are very abundant in the interstellar medium[1–3] and comets.[4,5] Photodissociation of these molecules by vacuum ultraviolet radiation is a major destruction process.[1,2] The quantum yields for various photodissociation products are important for determining the destruction rate of HCN and the formation rates of such fragments as H, C, CH, NH, and CN. The yields for the production of photofragment emissions are also important for the development of photodissociation lasers; for example, lasing from the CH ($A\,^2\Pi_i - X\,^2\Sigma^+$) system has been observed.[6,7] The photodissociation processes of HCN are also of fundamental interest. The vibrational populations of the CN ($B\,^2\Sigma^+$) fragments from HCN photodissociation are frequently used to test the theoretical models for the photodissociation mechanism of triatomic molecules.[8] The quantum yields for the production of various photofragments are important for the fundamental understanding of photodissociation processes.

There have been extensive investigations of the photoabsorption spectra[6,9–11] and electron excitation functions[12–15] of HCN in the energy region of 8–12 eV. The potential energies and geometries of the low-lying electronic states of HCN have been calculated by several authors.[16–20] In addition to the excitation of HCN itself, the fragmentation processes after its excitation have been also studied extensively.[10,21–27] Emissions from CN photofragments were first observed by Okabe and his associates.[21,22] They determined the H–CN bond energy from the threshold for the production of the CN ($B\,^2\Sigma^+ - X\,^2\Sigma^+$) emission,[21] and the vibrational population of the CN ($B\,^2\Sigma^+$) state from the emission spectra.[22] The vibrational population was further measured by Simons and co-workers[23] and Stein and Gedanken.[24] Chamberlain and Simons[25] also studied the polarization of the CN ($B\,^2\Sigma^+ - X\,^2\Sigma^+$) emission. In contrast to these studies, the CN ($A\,^2\Pi_i - X\,^2\Sigma^+$) emission from HCN photodissociation has been studied only occasionally.[10,22,26] The vibrational population in the CN($A\,^2\Pi_i$) state is not well known. There are few quantitative measurements for the production of the CN emissions, and the quantum yields have been measured only once. In this paper, the quantum yields for CN ($A\,^2\Pi_i$, $B\,^2\Sigma^+ - X\,^2\Sigma^+$) emissions from HCN photodissociation are reported in detail.

II. EXPERIMENTAL

The experimental setup has been described in a previous paper.[28] Briefly, the synchrotron radiation from the electron storage ring of the University of Wisconsin was used as the light source, which was dispersed by a 1 m vacuum monochromator (McPherson 225). The gas cell was separated from the vacuum monochromator by a LiF window at the exit slit. The photon flux passing through the gas cell was measured by a photodiode in the 1150–1600 Å region and by a copper detector in the 1050–1200 Å region. The photon flux starts at the LiF window cutoff and slowly increases to reach a maximum at 1250 Å. For a monochromator band width of 2 Å, the maximum photon flux is 5.5×10^7 photons/sec for each milliampere of electron beam current in the storage ring. The electron beam current is about 100 mA when it is freshly injected and decreases slowly with time.

The gas cell is 3.5 cm in diameter and 40 cm long. The emissions were observed by the combination of various optical filters and a cooled photomultiplier (EMI 9558QB) in a direction perpendicular to the primary photo beam. Figure 1 shows the relative responses (filter transmittance times photomultiplier quantum yield) for four filters: (1) Corning 7-54, (2) Corning 18A, (3) Oriel 3889 Å band, and (4) Corning 3-71. The filter transmittances were measured by a Cary recording spectrometer, and the photomultiplier quantum yield was adopted from the data given by EMI. The photon pulses from the photomultiplier were counted by an ORTEC counting system.

The HCN gas supplied by the Matheson Gas Company is 2.20% in helium. The gas was admitted into the gas cell without further purification. The helium gas does not absorb light in the present wavelength region. The absorptions from other impurities are small, because the photoabsorption bands for the possible impurities, such as N_2, O_2, and H_2O, are not shown in the present photoabsorption spectra. The gas pressure inside the

 0021-9606/80/126414-08$01.00

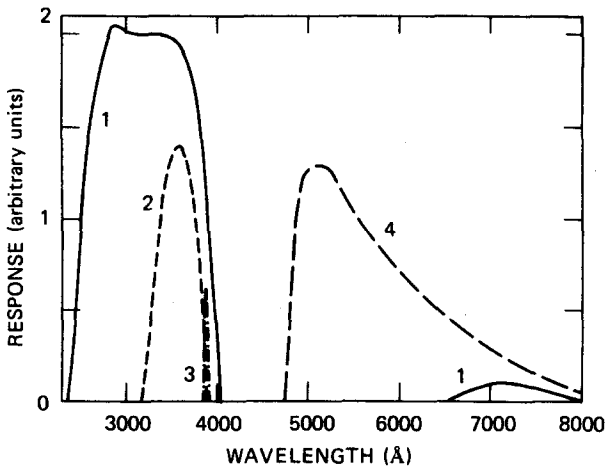

FIG. 1. The responses for the combination of a cooled photomultiplier (EMI 9558 QB) with four filters: (1) Corning 7-54, (2) Corning 18A, (3) Oriel 3889 Å band, and (4) Corning 3-71.

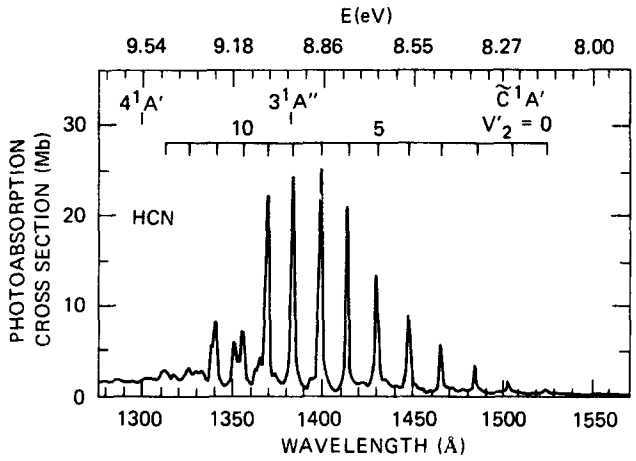

FIG. 3. The photoabsorption cross section of HCN in the 1275–1570 Å region. The positions for the electronic states of $3\,^1A''$ and $4\,^1A'$ calculated by Schwenzer *et al.* (Ref. 17) and these of $\tilde{C}\,^1A'$ assigned by Herzberg (Ref. 9) are indicated. The positions for the vibrational levels of the $\tilde{C}\,^1A'$ state are also shown.

gas cell was monitored with a Baratron capacitance manometer.

III. RESULTS

A. Photoabsorption cross section

The photoabsorption cross section of HCN has been measured only very recently.[10,11,27] In the present experiments, the cross section was measured by a method of photon flux attenuation, which was described in a previous paper.[28] The photoabsorption cross sections are shown in Fig. 2 for the 1050–1275 Å region and in Fig. 2 for 1275–1570 Å. The monochromator resolution in these measurements is set at 0.83 Å. The cross sections are in units of Mb ($=10^{-18}$ cm^2).

The measured photoabsorption cross section depends on the monochromator bandwidth.[29] The true molecular cross section is obtained only when the monochromator bandwidth is much smaller than the true molecular absorption bandwidth. For wavelengths shorter than 1350 Å, the molecular bandwidths are very broad, so the measured absorption cross sections are close to the true molecular photoabsorption cross sections. However, for the wavelengths longer than 1350 Å, discrete structures are observed, and the molecular bandwidths are in the same order of the monochromator bandwidth. Thus, the data shown in Fig. 3 are not equal to the true photoabsorption cross sections. The apparent cross sections for the 1398.5 Å band were measured at various monochromator bandwidths, and the results are shown in Fig. 4. The apparent cross

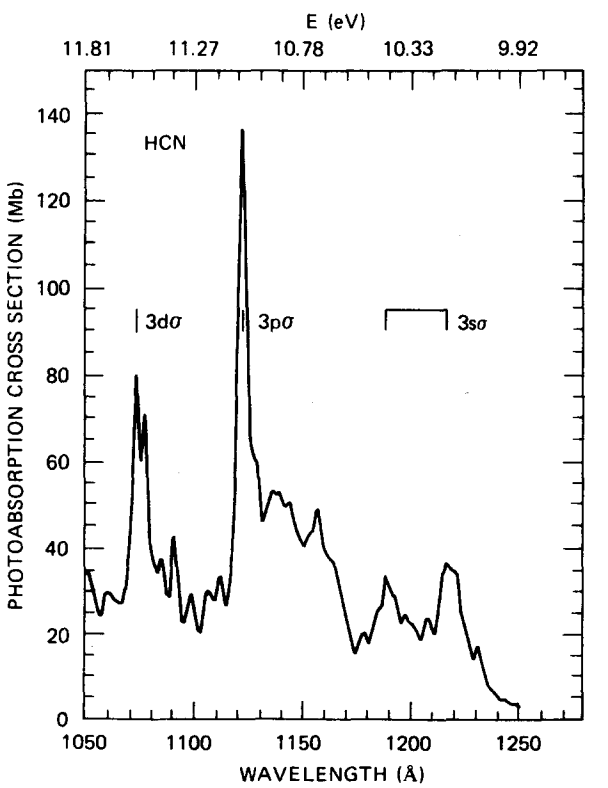

FIG. 2. The photoabsorption cross section of HCN in the 1050–1275 Å region. The cross sections are in units of Mb ($=10^{-18}$ cm^2). The positions for the Rydberg states assigned by Åsbrink *et al.* (Ref. 14) are indicated.

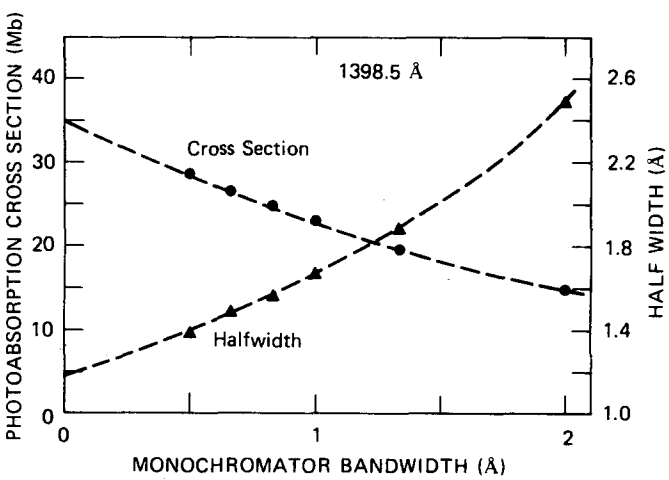

FIG. 4. The dependence of the photoabsorption cross section and the half-width on the monochromator bandwidth for the HCN ($\tilde{C}\,^1A'$ $v_2' = 7$) band at 1398.5 Å.

sections increase with decreasing monochromator bandwidths. The apparent cross section at a monochromator bandwidth of 0.83 Å is 25 Mb, but it increases to 35 Mb when extrapolated to zero monochromator bandwidth. The apparent molecular photoabsorption bandwidths versus the monochromator bandwidths are also shown in Fig. 4. The true molecular bandwidth is about 1.2 Å, when the monochromator bandwidth is extrapolated to zero.

In the 1300–1570 Å region, the present results agree very well with the previous measurements,[10,11,27] when the different monochromator bandwidths are taken into account. In the 1050–1300 Å region, the present data agree reasonably well with the measurements of West[10] and Glicker,[11] except at 1075 and 1123.5 Å, where the present values are 80 and 137 Mb in contrast to West's values of 65 and 84 Mb, respectively. In the measurements of West, the photon fluxes were measured by a combination of sodium salicylate UV converter and photomultiplier. Emissions from the excited CN photofragments (see next section) may transmit through the sodium salicylate-coated window to reach the photomultiplier, so the molecular absorption cross sections appear to be low. In the present measurements, the photon fluxes are measured by a copper detector, so the photofragment emissions are not detected. When the copper detector was replaced by a combination of sodium salicylate-coated window and photomultiplier, we found that the measured photoabsorption cross sections are lower than the values shown in Fig. 2.

The uncertainties in the present measurements are estimated to be less than 10% of the given values, where the uncertainties of 5% for the relative photon flux and 2% for pressure are included.

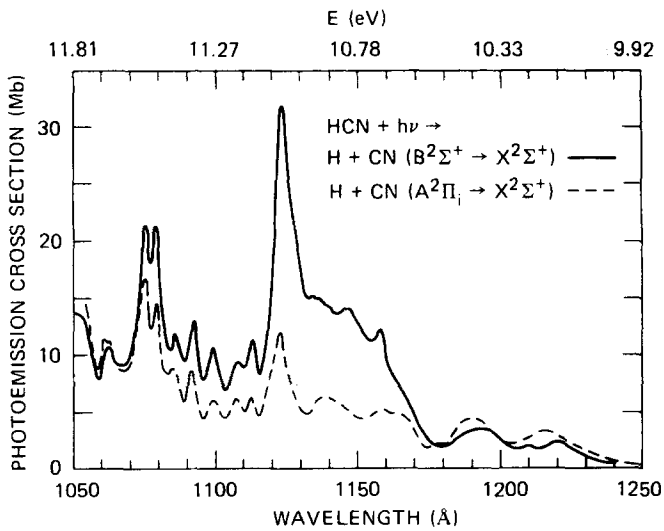

FIG. 5. The cross sections for the production of $CN(A\,^2\Pi_i \rightarrow X\,^2\Sigma^+)$ and $CN(B\,^2\Sigma^+ \rightarrow X\,^2\Sigma^+)$ emissions from HCN photodissociation in the 1050–1250 Å region. The $CN(A\,^2\Pi_i \rightarrow X\,^2\Sigma^+)$ emission is isolated by Filter 4 and $CN(B\,^2\Sigma^+ \rightarrow X\,^2\Sigma^+)$ by Filter 1. The cross section for $CN(A\,^2\Pi_i \rightarrow X\,^2\Sigma^+)$ emission represents only a lower limit. The cross sections were measured at HCN pressure lower than 10 mtorr. The cross sections for the production of $CN(A\,^2\Pi_i \rightarrow X\,^2\Sigma^+)$ and $CN(B\,^2\Sigma^+ \rightarrow X\,^2\Sigma^+)$ emissions from HCN photodissociation in the 1275–1480 Å region. The cross sections were measured at HCN pressure lower than 10 mTorr.

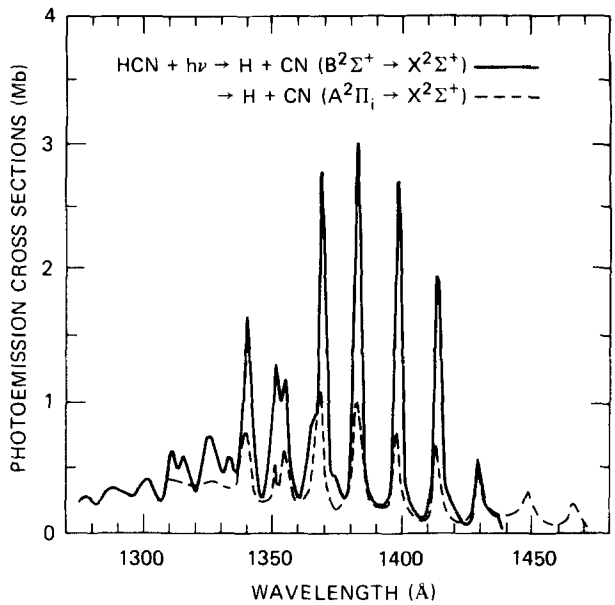

FIG. 6. The cross sections for the production of $CN(A\,^2\Pi_i \rightarrow X\,^2\Sigma^+)$ and $CN(B\,^2\Sigma^+ \rightarrow X\,^2\Sigma^+)$ emissions from HCN photodissociation in the 1275–1480 Å region. The cross sections were measured at HCN pressure lower than 10 mTorr.

B. Photoemission cross sections

The partial cross sections for the production of $CN\,(B\,^2\Sigma^+ \rightarrow X\,^2\Sigma^+)$ and $CN\,(A\,^2\Pi_i \rightarrow X\,^2\Sigma^+)$ emissions from HCN photodissociation were measured from their emission rates. At low gas pressure, the emission rate is given[28] by

$$\dot{n}_f = CF\,\sigma_f I_0 n \qquad (1)$$

where C is a geometrical constant, F is the detection response shown in Fig. 1, σ_f is the cross section for photoemission, I_0 is the photon flux of synchrotron radiation, and n is the gas density. Equation (1) is valid only when the loss of the excited fragments due to quenching can be neglected. This is justified by the fact that the emission rate is linearly dependent on the gas pressure up to 10 mTorr of HCN. The geometrical constant is determined by the OH $(A\,^2\Sigma^+ \rightarrow X\,^2\Pi_i)$ emission from the H_2O photodissociation, for which the photoemission cross section is known.[28] The results for both the emission systems are described below.

The vibrational populations for the CN $(B\,^2\Sigma^+)$ fragment produced from HCN photodissociation are in the $v' \leq 4$ vibrational levels.[22–24] The emission for this system in the 3800–3890 Å region was isolated by Filter 1 (Fig. 1). The OH $(A\,^2\Sigma^+ \rightarrow X\,^2\Pi_i)$ emission was also isolated by the same filter, so the uncertainties resulting from the detection systems were minimized. The detection response is averaged over the emission spectrum, which is equivalent to the response near 3870 Å. The cross sections for the production CN $(B\,^2\Sigma^+ \rightarrow X\,^2\Sigma^+)$ emission from HCN photodissociation are shown in Fig. 5 for the wavelength region of 1050–1250 Å and in Fig. 6 for 1275–1450 Å, where the monochromator bandwidth is 2 Å.

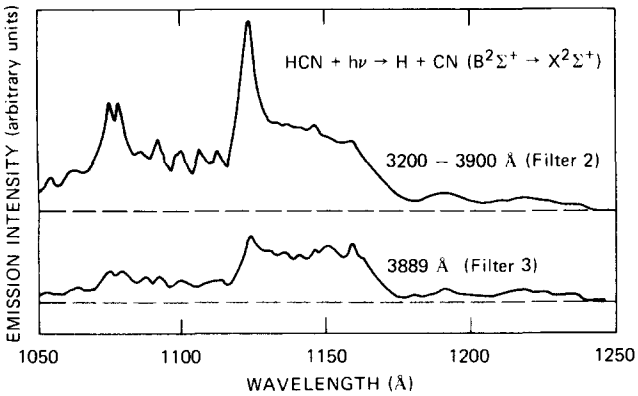

FIG. 7. The excitation functions for the CN($B^2\Sigma^+ \rightarrow X^2\Sigma^+$) emission isolated by Filters 2 and 3. The coordinates are the emission radiation rates.

The uncertainties for the cross sections are estimated to be less than 40%, which is mainly a result of the uncertainty in the OH ($A^2\Sigma^+ - X^2\Pi_i$) emission. Because the photoabsorption cross section in the 1240–1280 Å region is very small, the cross sections for photoemission are also small and are not measured. Although Filter 1 has a low response in the 7000 Å region, this may not seriously affect the observed CN ($B^2\Sigma^+ - X^2\Sigma^+$) emission rate because the contribution from the possible emission of the CN ($A^2\Pi_i - X^2\Sigma^+$) system in this wavelength region is small. This is corroborated by the fact that the excitation functions obtained from Filters 1 and 2 are the same. Filter 2 has very low transmission in the IR region.

As shown in Fig. 6, the CN ($B^2\Sigma^+ - X^2\Sigma^+$) emission begins to have a significant cross section at 1439 Å, although the threshold has been observed to be at 1475 Å.[21] The photoemission cross section spectrum is very similar to the photoabsorption cross section, except in the 1175–1250 Å region where the photoemission cross section is relatively small. The 1075 and 1123 Å bands, which are assigned to the Rydberg states,[14] are mainly due to emissions from highly excited vibrational levels. This is suggested by the fact that when the emissions are isolated by a narrow band filter (No. 3), which transmits only the emission from the $v' = 0 - v'' = 0$ band, these two bands disappear as shown in Fig. 7. The excitation spectra isolated by Filters 2 and 3 are compared in Fig. 7. Filter 2 includes the emissions from all the vibrational levels of the CN ($B^2\Sigma^+$) state, but the Filter 3 transmits the emission mainly from the $v' = 0$ level (see Sec. IV-C for further discussion).

The vibrational population for CN ($A^2\Pi_i$) fragments from HCN photodissociation are not well known. Tereschenko and Dodonova[26] estimated that the vibrational populations decrease monotonically with increasing vibrational level. This indicates that the emission will spread from visible to near infrared. Since the wavelength region isolated by Filter 4 (Fig. 1) is only a fraction of total emission spectrum, the cross section reported here for the CN ($A^2\Pi_i - X^2\Sigma^+$) emission from HCN photodissociation is viewed only as a lower limit. Because the spectrum of the CN ($A^2\Pi_i - X^2\Sigma^+$) emission from HCN photodissociation is not known, the detection response for this system cannot be determined accurately. The measured radiation rate is converted to the cross section using the average response of Filter 4, which is equivalent to the value at 6100 Å. The cross sections are shown in Fig. 5 for the 1050–1250 Å region and in Fig. 6 for 1275–1470 Å.

Taking the threshold for the production of the CN ($B^2\Sigma^+$, $v' = 0$) photofragment to be at 1475 Å,[21] the threshold for the production of CN ($A^2\Pi_i$, $v = 0$) will be at 1950 Å, where the electronic energies[30] for the CN ($A^2\Pi_i$ and $B^2\Sigma^+$) states are 9241.66 and 25 751.8 cm^{-1}, respectively. The photon energies reported here are sufficiently energetic to produce the CN ($A^2\Pi_i$) fragments excited in the high vibrational levels. Emission from the $v' = 10$ level has been observed.[26] The emissions observed here are mainly from the high vibrational levels, in contrast to West's measurements that are limited to the emissions from low vibrational levels of the CN ($A^2\Pi_i$) state.

C. Quantum yields

The quantum yield is defined as the ratio of the photoemission cross section to the photoabsorption cross section. Both the photoemission and photoabsorption cross sections need to be measured at an equivalent monochromator bandwidth, because the cross section is affected by the monochromator bandwidth (see Fig. 4). The photoabsorption cross sections reported here were measured at a monochromator bandwidth of 0.83 Å, but photoemission cross sections were measured at 2 Å. In the 1050–1250 Å region, the molecular bandwidths are very broad, so the cross sections are not seriously affected by the monochromator bandwidth. Therefore, the photoabsorption and photoemission cross sections shown in Fig. 2 and Fig. 5 are used to calculate the quantum yields without correction. However, in the 1300–1470 Å region, the molecular bandwidths are narrow, so the photoabsorption cross sections at the band peaks are corrected to the values at a monochromator bandwidth of 2 Å. The quantum yields for CN ($B^2\Sigma^+ - X^2\Sigma^+$) emission produced from HCN photodissociation are shown in Fig. 8 and for CN ($A^2\Pi_i - X^2\Sigma^+$) emission in Fig. 9. In the 1275–1500 Å region the quantum yields are determined only

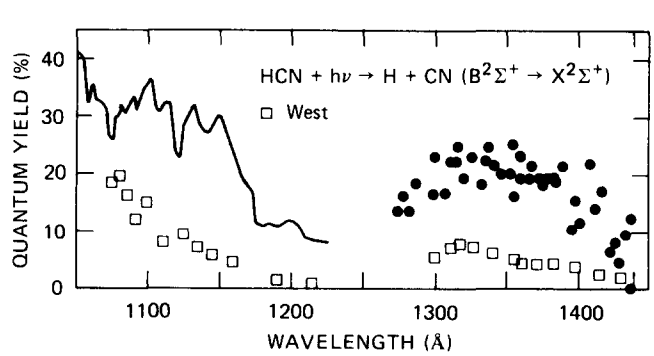

FIG. 8. The quantum yield for the production of CN($B^2\Sigma^+ \rightarrow X^2\Sigma^+$) emission from HCN photodissociation. The data given by West (Ref. 10) are indicated for comparison.

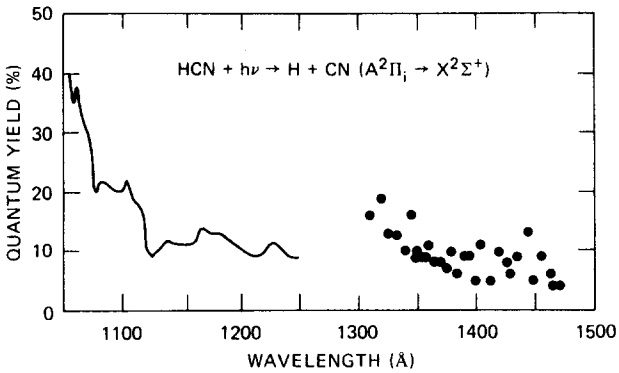

FIG. 9. The quantum yield for the production of CN($A\,^2\Pi_i \rightarrow X\,^2\Sigma^+$) emission from HCN photodissociation.

at the wavelengths of photoabsorption maxima and minima.

The quantum yields for CN ($B\,^2\Sigma^+ \rightarrow X\,^2\Sigma^+$) emission are about 30% for the wavelengths in the 1050–1150 Å region, 10% in 1180–1230 Å, and 20% in 1300–1400 Å. These data are much higher than the values given by West,[10] which are also shown in Fig. 8 for comparison. The discrepancy may be in part due to the different calibration techniques. In West's measurements, the quantum yields are obtained by calibration against SO_2 fluorescence excited at 2206 Å, but the values reported here were obtained by calibration against the OH ($A\,^2\Sigma^+ \rightarrow X\,^2\Pi_i$) emission from H_2O photodissociation in the 1050–1370 Å region. In the present measurements both the CN ($B\,^2\Sigma^+ \rightarrow X\,^2\Sigma^+$) and OH ($A\,^2\Sigma^+ \rightarrow X\,^2\Pi_i$) emissions are excited by the same photon wavelengths and detected by the same detection system, so the experimental uncertainties are greatly reduced.

The quantum yields for CN ($A\,^2\Pi_i \rightarrow X\,^2\Sigma^+$) emission are about 40% at 1060 Å and then decrease to about 10% for wavelengths longer than 1120 Å. These yields are for the emissions from high vibrational levels that were not previously measured. West[10] determined the quantum yields for the emissions from the low vibrational levels to be about 15%.

IV. DISCUSSION

A. Electronic states

The electronic states of HCN have been investigated by several authors.[9,12,14,16,17] HCN in the ground state[9] is linear and has an electronic configuration of $1\sigma^2 2\sigma^2 3\sigma^2 4\sigma^2 1\pi^4$. Since most of the excited electronic states are bent, it is convenient to consider the ground electronic state in a bent geometry with an electronic configuration[17] of $1a'^2 2a'^2 3a'^2 4a'^2 5a'^2 6a'^2 1a''^2$. The electronic states in the energy region reported here are formed by exciting electrons from the occupied orbitals of $5a'$, $6a'$, and $1a''$ to the empty orbitals of $7a''$, $2a''$, and $8a'$. The positions for the electronic states calculated by Schwenzer *et al.*[17] are indicated in Fig. 3. The experimental measurements are compared with the theoretical calculations as follows.

The $3\,^1A'$ state calculated by Schwenzer *et al.*[17] has the energy of 7.85 eV (1579 Å), corresponding to the $\tilde{C}\,^1A'$ state assigned by Herzberg.[9] This state has a long progression of bending vibration, for which the positions of absorption peaks are listed in Table I. These positions agree very well with the measurements of MacPherson and Simons,[27] which are also listed in Table I for comparison. As shown in Table I, the vibrational frequencies are about 860 cm^{-1} for $v_2' \leq 5$, and then decrease at high vibrational levels to less than 810 cm^{-1}. The decrease of vibrational frequencies for $v_2' = 5$–9 may indicate that these vibrational structures are formed by a photoabsorption process different from those for $v_2' < 5$ levels. At the $v_2' = 5$ level (Table I), the CN ($B\,^2\Sigma^+ \rightarrow X\,^2\Sigma^+$) emission starts to have a high cross section (Fig. 6). These vibrational structures may be due to same vibrational mode that has been designated to the HCN bending mode,[9] but the high vibrational levels may be perturbed by some other states. In addition to the intense absorption features, weak bands are distributed in the 1400–1530 Å region and are attributed to the hot band absorption of HCN originating in the $\tilde{X}\,^1\Sigma^+$ (0, 1, 0) bending vibrational level.[9]

As shown in Fig. 3, the photoabsorption cross section drops sharply at $v_2' \geq 10$ and the vibrational frequencies become irregular. This irregularity has been interpreted[14] as evidence for the existence of the linear $3\,^1A''$ state,[17] but has been reinterpreted[20] to be a result of a simultaneous excitation of the bending and stretching modes. Some of the irregular bands are assigned by MacPherson and Simons[27] to the (0, v_2', 1) progression. The HC–N stretching frequency v_3' obtained from this assignment is about 1650–1750 cm^{-1}. Although these assignments seem reasonable, there remains a question of why the stretching mode only occurs at high bending vibrational levels. Therefore, the previous interpretation that the $\tilde{C}\,^1A'$ state is perturbed by the $3\,^1A''$ (or $\tilde{D}$) state[9,17] can not be ruled out. It has been stated[20] that the $3\,^1A''$ state can not be photoexcited from the ground state. However, this state may perturb the potential surface of the $\tilde{C}\,^1A'$ state, so that the vibrational structures are accordingly changed.

The $4\,^1A'$ state has a calculated[17] excitation energy of

TABLE I. Positions for the peaks of the HCN ($\tilde{C}\,^1A'$, $0v_2'0 \leftarrow \tilde{X}\,^1\Sigma^+$, 000) transitions.

V_2'	λ (Å)	ν_2' (cm^{-1})	$\Delta\nu_2$ (cm^{-1})	ν_2' (cm^{-1})[a]
0	1523.3	65647		
			873	
1	1503.3	66520		
			856	
2	1484.2	67376		
			851	
3	1465.7	68227		
			858	
4	1447.5	69085		69085
			855	69950
5	1429.8	69940		
			806	70750
6	1413.5	70746		
			769	71515
7	1398.3	71515		
			775	72280
8	1383.3	72290		
			751	73035
9	1369.1	73041		
			705	73770
10	1356.0	73746		
			809	74570
11	1341.3	74555		
			877	75370
12	1325.7	75432		
			782	
13	1312.1	76214		

[a]From Ref. 27.

9.54 eV (1299 Å). This state is linear and is mainly due to the $6a' \rightarrow 8a'$ orbital excitation. As shown in Figs. 2 and 3, this calculated excitation energy is near the absorption band at 1218 Å. Chutjian *et al.*[15] assigned the $4\,^1A'$ state to the 1218 Å band, but it was recently reassigned to the absorption band at 1140 Å by Åsbrink *et al.*[14] The CN ($B\,^2\Sigma^+ - X\,^2\Sigma^+$) yield reported here shows a minimum near 1200 Å, indicating that there exists a state. Since this state has an energy very close to the calculated energy for the $4\,^1A'$ state, it is likely that they are the same state.

The quantum yields for emissions from photofragments are useful to indicate the existence of excited states. As mentioned above, the low CN ($B\,^2\Sigma^+ - X\,^2\Sigma^+$) yield in the 1180–1259 Å region (Fig. 8) indicates that a state exists. Similarly, the quantum yields for the CN ($A\,^2\Pi_i - X\,^2\Sigma^+$) emission are approximately constant at 21% and 11% for the 1075–1115 Å and the 1125–1165 Å regions (Fig. 9), respectively. These results indicate that different states exist in these regions. Weak vibrational structures are superimposed on these absorption continua. These weak structures may result from excitations into vibrational levels of bound states, which then predissociate. Recently, Vazquez and Gouyet[31] have calculated the potential curves for H–CN dissociation, which show several bound states in these energy regions. Alternatively, these vibrational structures may result from the dissociation mechanisms proposed by Pack[32] and Heller.[33] In some cases diffuse vibrational structures will be superimposed on the photodissociation continua of symmetric triatomic molecules, because of an oscillation in a symmetrical coordinate before dissociation. Such phenomena may be applicable[32,33] to the photodissociation of unsymmetric molecules.

The symmetries for the states in the 1080–1115, 1130–1170, and 1175–1250 Å regions may be identifiable by the polarization of CN emission. The lifetimes for HCN existing in these states may be short, which can be estimated from the oscillation period of vibration in a bound coordinate. For example, the average vibrational frequency for the structure in the 1080–1115 Å region is $\Delta\nu = 550\ \text{cm}^{-1}$ ($= 1.65 \times 10^{13}\ \text{sec}^{-1}$) so the oscillation period is about 6×10^{-14} sec. The HCN molecules in the excited state may exist not much longer than this oscillation period. Because this lifetime is shorter than the molecular rotational period of about 2×10^{-13} sec,[27] the CN photofragment emission may be polarized. The emission polarization can in turn be used to determine the symmetry of a molecular state.[25,34]

B. Photodissociation processes

When an HCN molecule is excited by a high energy photon, it will decay through various competitive channels. Dissociations into the excited products of CN ($A\,^2\Pi_i$) and CN ($B\,^2\Sigma^+$) are apparently the major channels because their quantum yields are quite high. The quantum yields for CN ($B\,^2\Sigma^+$) production are about 20% in the 1270–1450 Å region, 10% in 1170–1250 Å, and 30% in 1050–1150 Å (Fig. 8). The quantum yields

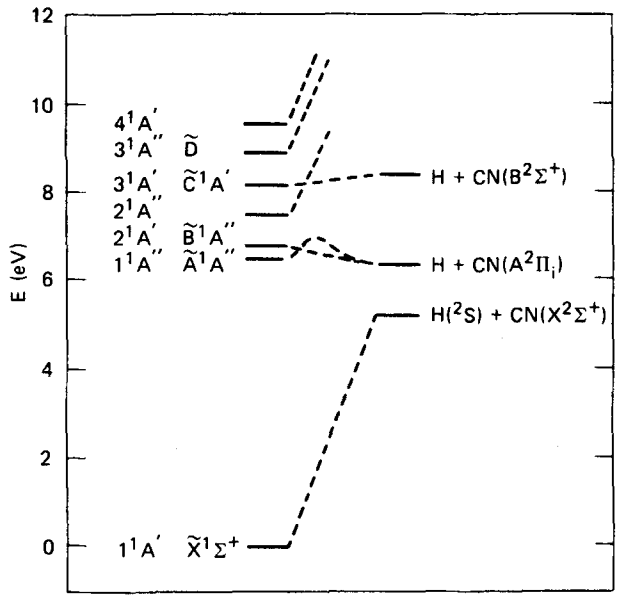

FIG. 10. The adiabatic correlation diagram for the HCN electronic states to various dissociation limits.

for the CN ($A\,^2\Pi_i$) production shown in Fig. 9 represent only the emissions from the high vibrational levels and are considered as a lower limit. The yield from the production of the CN ($A\,^2\Pi_i$) in low vibrational levels[10] is about 15%. For photon wavelengths shorter than 1130 Å, the sum of the CN ($A\,^2\Pi_i$) and CN ($B\,^2\Sigma^+$) production yields are larger than 65%. However, at longer wavelengths, the total measured yields account for only 45%. Dissociation of HCN into H + CN ($X\,^2\Sigma^+$) may be the additional major channel. The yield for the HCN molecular emissions from the highly excited states are expected to be small because the lifetimes in the molecular excited states are very short compared with the typical radiative lifetime.

The processes for dissociating HCN into various products will be better understood through a correlation diagram as shown in Fig. 10, where the states designated by Herzberg[9] are indicated with characters and those of Schwenzer *et al.*[17] with numbers. The $\tilde{A}\,^1A''$ state has a potential barrier in the CH stretch.[18] Recent theoretical calculations show that the $\tilde{B}$ state is more likely to have $^1A'$ symmetry,[17,18] instead of $^1A''$ originally assigned by Herzberg and Innes.[35] However, Herzberg[36] believes that the rotational structure shows quite unambiguously that this state is $^1A''$. The $\tilde{A}$ and $\tilde{B}$ states are correlated to H + CN ($A\,^2\Pi_i$)[6,31,35] and $\tilde{C}$ to H + CN ($B\,^2\Sigma^+$).[6,31] The $2\,^1A''$, $3\,^1A''$, and $4\,^1A'$ states are bound in the H–CN coordinate.[31] It is energetically possible to dissociate the HCN molecules into H + CN ($A\,^2\Pi_i$, $B\,^2\Sigma^+$, and $X\,^2\Sigma^+$) by photon energies reported here (8–11.8 eV).

The correlation of the $\tilde{C}\,^1A'$ state to H + CN ($B\,^2\Sigma^+$) (Fig. 10) brings up the question of how the $\tilde{C}\,^1A'$ state maintains a long progression of vibrational states of energies beyond the dissociation limit as shown in Figs. 3 and 6. A simple explanation is to assume that the $\tilde{C}\,^1A'$ state has a potential barrier beyond the dissociation limit similar to the $\tilde{A}\,^1A''$ state, so the

bound states are maintained within the potential well. This assumption of a potential barrier needs to be substantiated by further theoretical calculations. The dissociation at the discrete states is through a predissociation process, which results from the interaction of the discrete states with dissociation continua. The predissociation process has been discussed in several papers[9,37] and is well understood. Nevertheless, these general theoretical descriptions have not been applied to a specific molecule such as HCN. The coupling strengths among the discrete states and various dissociation continua have not been calculated.

The vibrational structures in the 1080–1120 and the 1130–1170 Å regions can not be attributed to the vibrationally excited Rydberg states. The vibrational structures in the 1130–1170 Å region could be naively assigned to the vibrational excitation of the $3s\sigma$ Rydberg state in the 1180–1250 Å region. However, the CN ($B-X$) quantum yields for the structures are very different from those for the Rydberg states (Fig. 8); so they belong to different states. Similarly, the CN ($A\,^2\Pi_i - X\,^2\Sigma^+$) emission yields for the 1080–1120 Å bands (Fig. 9) are different from that for the 1123 Å Rydberg state, so the structures in the 1080–1120 Å region are not the vibrational excitation of the $3p\sigma$ Rydberg state. The weak structure distributed in the 1080–1250 Å region may be attributable to the vibrational levels of the bound molecular states[31] in this energy region.

C. Vibrational excitation

The quantum yield for dissociating into a specific electronic state is mainly determined by the potential surface of the initial excited state. The internal energy in the electronic state will be redistributed by the interaction dynamics during the fragmentation period. Thus, the vibrational population of a diatomic photofragment depends both on the initial Franck–Condon transition and on the interaction among the dissociation products during fragmentation. Several investigators[22–24] have measured the vibrational populations of the CN ($B\,^2\Sigma^+$) fragments from HCN photodissociation to test various theoretical models.[8] Nevertheless, the vibrational populations were measured only at a few wavelengths, and the existing data were not enough to support the theoretical modeling of the photodissociation dynamics. More data for the vibrational populations of the diatomic photofragments produced from both the direct dissociation and predissociation processes are needed for further understanding of the photodissociation mechanism. For this purpose, we isolate the CN ($B\,^2\Sigma^+ - X\,^2\Sigma^+$) emissions from different vibrational levels by filters, and their excitation functions are shown in Fig. 7.

It is clear from Fig. 7 that the CN ($B\,^2\Sigma^+$) fragments produced by the Rydberg states are more populated at high vibrational levels than those produced by the other dissociative states. The molecules excited in a Rydberg state may live longer than those in other dissociative states so that the vibrational populations produced by the Rydberg states are more affected by the final interaction between H and CN ($B\,^2\Sigma^+$) during fragmentation. The final interaction[38] will excite the diatomic photofragments from low to high vibrational levels. Therefore, the photofragments produced by Rydberg states will be more vibrationally excited. An alternative explanation for the high vibrational excitation in the Rydberg transition is that the excited state is linear. High vibrational excitations have been observed in several diatomic photofragments produced by photodissociation of linear triatomic molecules.[39] The present results clearly demonstrate that the vibrational populations of the CN ($B\,^2\Sigma^+$) fragments depend on the dissociation processes.

V. CONCLUDING REMARKS

The mechanism for producing the vibrational structures in the $\tilde{C}\,^1A'$ state beyond the H + CN ($B\,^2\Sigma^+$) limit needs to be further investigated. The vibrational structures may be caused by a potential barrier in the $\tilde{C}\,^1A'$ state. The cause for the irregularity at the high vibrational level of $v_2' \geq 10$ is not known with certainty. Earlier reports[5,14] attributed this irregularity to a new state entering in this energy region, but was recently reattributed to the asymmetrical stretch.[20,27] A present argument favors the earlier reports that the irregularity is caused by the potential surface of the $\tilde{C}\,^1A'$ state being perturbed by a new state, $3\,^1A''$ or $\tilde{D}$.

Three states of HCN in the 1080–1115 Å, 1130–1170 Å, and 1175–1250 Å regions are found from the quantum yields for the production of the CN ($A\,^2\Pi_i - X\,^2\Sigma^+$) and CN ($B\,^2\Sigma^+ - X\,^2\Sigma^+$) emissions. The state in the 1175–1250 Å region is probably the $4\,^1A'$ state,[15] but the symmetries for the other two states are not known. Their symmetries can be determined by the polarization of the CN emissions. Vibrational structures superimposed on these states are observed.

The sum of the quantum yields for the production of the CN ($A\,^2\Pi_i$) and CN ($B\,^2\Sigma^+$) fragments from HCN photodissociation are larger than 0.65 for the photon wavelengths shorter than 1130 Å, but are less than 0.45 for the longer wavelengths. In the long wavelength region, HCN molecules may also photodissociate into CN fragments in the ground state.

ACKNOWLEDGMENTS

The author wishes to thank Professor J. T. Moseley for initial collaboration on this research program. He also wishes to thank Dr. D. L. Huestis for helpful discussion and Dr. E. J. Heller, Dr. G. Herzberg, Dr. R. T Pack, and Ms. J. A. Guest for helpful comments. He is grateful to the staff of the Synchrotron Radiation Center of the University of Wisconsin for providing the facility, particularly E. M. Rowe and R. Otte. The use of the monochromator belonging to Professors Z. Hurych and D. L. Benbow of the Northern Illinois University (supported by NSF Grant DMR-78-11663) is acknowledged. The Synchrotron Radiation Facility is supported by the National Science Foundation under Contract No. DMR-77-21888.

This work was supported by the National Aeronautics and Space Administration/Astrophysics Division under Contract No. NASW-3270.

[1]A. Dalgarno and J. H. Black, Rep. Prog. Phys. **39**, 573 (1976).
[2]W. D. Watson, Rev. Mod. Phys. **48**, 513 (1976).
[3]B. E. Turner and P. Thaddeus, Astrophys. J. **211**, 755 (1977); P. J. Huggins, T. G. Phillips, G. Neugebauer, M. W. Werner, P. G. Wannier, and D. Ennis, Astrophys. J. **227**, 441 (1979); A. A. Penzias, Astrophys. J. **228**, 430 (1979); A. A. Stark and R. S. Wolff, Astrophys. J. **229**, 118 (1979).
[4]W. M. Jackson, J. Photochem. **5**, 107 (1976).
[5]J. B. Tatum and M. J. Gillespie, Astrophys. J. **218**, 569 (1977).
[6]G. A. West and M. J. Berry, J. Chem. Phys. **61**, 4700 (1974).
[7]V. I. Korol and S. M. Kishko, Opt. Spectrosc. **38**, 486 (1975); C. R. Quick, Jr., C. Wittig, and J. B. Laudenslager, Opt. Commun. **18**, 268 (1976).
[8]For example, M. J. Berry, Chem. Phys. Lett. **29**, 329 (1974); S. Mukamel and J. Jortner, J. Chem. Phys. **60**, 4760 (1974); Y. B. Band and K. F. Freed, J. Chem. Phys. **63**, 3382 (1975); *ibid.* **67**, 1462 (1977); O. Atabek, J. A. Beswick, R. Lefebvre, S. Mukamel, and J. Jortner, J. Chem. Phys. **65**, 4035 (1976); J. A. Beswick, M. Shapiro, and R. Sharon, J. Chem. Phys. **67**, 4045 (1977); O. Atabek and R. Lefebvre, J. Chem. Phys. **67**, 4983 (1977).
[9]G. Herzberg, *Electronic Spectra of Polyatomic Molecules* (Van Nostrand, New York, 1966).
[10]G. A. West, Ph.D. Thesis, University of Wisconsin, Madison, WI (1975).
[11]S. Glicker (private communication).
[12]W. C. Tam and C. E. Brion, J. Elect. Spectrosc. Rel. Phen. **3**, 281 (1974).
[13]A. P. Hitchcock and C. E. Brion, Chem. Phys. **37**, 319 (1979).
[14]C. Fridh and L. Åsbrink, J. Elect. Spectrosc. Rel. Phen. **7**, 119 (1975); L. Åsbrink, C. Fridh, and E. Lindholm, Chem. Phys. **27**, 159 (1978).
[15]A. Chutjian, H. Tanaka, B. G. Wicke, and S. K. Srivastava, J. Chem. Phys. **67**, 4835 (1977).
[16]I. Absar and K. L. McEwen, Can. J. Chem. **50**, 653 (1972).
[17]G. M. Schwenzer, S. V. O'Neil, H. F. Schaefer III, C. P. Baskin, and C. F. Bender, J. Chem. Phys. **60**, 2787 (1974); also, G. M. Schwenzer, C. F. Bender, and H. F. Schaefer III, Chem. Phys. Lett. **36**, 179 (1975).
[18]M. Peric, S. D. Peyerimhoff, and R. J. Buenker, Can. J. Chem. **55**, 3664 (1977).
[19]A. Rauk and J. M. Barriel, Chem. Phys. **25**, 409 (1977); also, G. J. Vazquez and J. F. Gouyet, Chem. Phys. Lett. **57**, 385 (1978).
[20]H. Koppel, L. S. Cederbaum, W. Domcke, and W. Von Niessen, Chem. Phys. **37**, 303 (1979).
[21]D. D. Davis and H. Okabe, J. Chem. Phys. **49**, 5526 (1968).
[22]A. Mele and H. Okabe, J. Chem. Phys. **51**, 4798 (1969).
[23]M. N. R. Ashfold, M. T. MacPherson, and J. P. Simons, Chem. Phys. Lett. **55**, 84 (1978).
[24]I. Stein and A. Gedanken, J. Chem. Phys. **68**, 2982 (1978).
[25]G. A. Chamberlain and J. P. Simons, J. Chem. Soc. Faraday Trans. II **71**, 2043 (1975).
[26]E. N. Tereschenko and N. Y. Dodonova, Opt. Spectrosc. **41**, 286 (1976).
[27]M. T. MacPherson and J. P. Simons, J. Chem. Soc. Faraday Trans. II **74**, 1965 (1978).
[28]L. C. Lee, J. Chem. Phys. (in press).
[29]R. D. Hudson, Rev. Geophys. Space Phys. **9**, 305 (1971).
[30]G. Herzberg, *Spectra of Diatomic Molecules* (Van Nostrand, Toronto, 1967), p. 520.
[31]G. J. Vazquez and J. F. Gouyet, Chem. Phys. Lett. **65**, 515 (1979).
[32]R. T Pack, J. Chem. Phys. **65**, 4765 (1976).
[33]E. J. Heller, J. Chem. Phys. **68**, 3891 (1978).
[34]M. T. McPherson, J. P. Simons, and R. N. Zare, Mol. Phys. **38**, 2049 (1979).
[35]G. Herzberg and K. K. Innes, Can. J. Phys. **35**, 842 (1957).
[36]G. Herzberg, private communication (1979).
[37]For example, S. A. Rice, J. McLaughlin, and J. Jortner, J. Chem. Phys. **49**, 2756 (1968); O. K. Rice, J. Chem. Phys. **53**, 439 (1971); C. E. Caplan and M. S. Child, Mol. Phys. **23**, 249 (1972); K. G. Kay, J. Chem. Phys. **60**, 2370 (1974); E. J. Heller and S. A. Rice, J. Chem. Phys. **61**, 936 (1974).
[38]K. E. Holdy, L. C. Klotz, and K. R. Wilson, J. Chem. Phys. **52**, 4588 (1970); F. E. Heidrich, K. R. Wilson, and D. Rapp, J. Chem. Phys. **54**, 3885 (1971).
[39]L. C. Lee and D. L. Judge, Can. J. Phys. **51**, 378 (1973); also, J. Chem. Phys. **63**, 2782 (1975).